



Strength Properties Petroleum Sludge/One-Part Geopolymer Mortar for Construction Properties

Salahu Hamza¹, Muhammad Bello Ibrahim¹, Sarki Aliyu Salisu¹, Basiru Abdussalam¹, Abubakar M. Abdullahi¹, Aliyu Usman², Nura Bala³

¹Dept. of Civil Engineering, School of Engineering, Hussaini Adamu Federal Polytechnic, Kazaure

²Dept. of Civil Engineering, Faculty of Engineering, Ahmadu Bello University, Zaria

³Dept. of Civil Engineering, Faculty of Engineering, Bayero University, Kano

*muhammad_17006885@utp.edu.my

ABSTRACT:

Geopolymer concrete, hailed for its sustainability compared to traditional Portland cement-based concrete, boasts a reduced carbon footprint and superior mechanical characteristics. This research delves into the strength attributes of one-part geopolymer concrete mortar mixed with petroleum sludge to specifically check its compressive, tensile, and flexural strengths. The experimental agenda entails formulating a one-part geopolymer concrete mortar utilizing fly ash as the principal binder, alongside alkaline activators. Diverse mix designs are crafted, manipulating factors like the fly ash to alkaline activator ratio, curing temperature, and duration. Compressive strength tests adhere to ASTM standards, while appropriate methodologies gauge tensile and flexural strengths. The impact of varied curing protocols on strength property evolution is scrutinized to refine mix designs for practical use. Findings underscore the viability of producing robust geopolymer concrete mortar with a simplified one-part formulation, heralding promising avenues for sustainable construction methodologies.

Introduction

Currently, the global pursuit of sustainable development is prompting the exploration of alternatives in construction materials. Geopolymer concrete emerges as a promising substitute capable of substantially reducing carbon dioxide emissions. Its production yields environmentally friendly concrete, offering a viable alternative to traditional OPC concrete. Traditional geopolymer mixes, requiring high-temperature curing, have been limited to precast structural elements. Previous research predominantly focused on heat-cured concretes using aggressive chemical activation processes, such as concentrated sodium hydroxide and sodium silicate. Consequently, there's a demand for novel geopolymer binders. The introduction of one-part geopolymer binders, employing a simple "just add water" method akin to ordinary Portland cement, presents an innovative solution. This study seeks to develop an ambient-cured one-part geopolymer binder suitable for in-situ casting at room temperature, addressing challenges associated with handling large quantities of alkaline solutions and elevated temperature curing. Preliminary results indicate that a fly ash blended slag one-part geopolymer demonstrates promising workability, density, and compressive strength. Incorporating slag with fly ash enhances compressive strength comparably to two-part geopolymer systems. Therefore, one-part geopolymer binders have the potential to enhance the commercial viability and widespread adoption of geopolymer concrete within the construction industry.

Currently, advancements in science and technology persist in enhancing global infrastructure. Innovations in the construction sector continually strive to identify low-carbon products for safer, more economical, and environmentally sustainable infrastructure designs. The demand for concrete is escalating with the rise in shelter and economic activities, fueled by globalization and industrialization, which heavily rely on concrete-based infrastructures. Ordinary Portland Cement (OPC) serves as a primary binder in conventional concrete production, but its production involves significant carbon dioxide emissions, exacerbating environmental concerns. To mitigate these emissions and address the growing demand for concrete, there is a pressing need to explore alternative materials with lower CO₂ footprints.

Geopolymer concrete presents itself as a promising solution. Unlike OPC-based concrete, geopolymer concrete production doesn't require OPC; instead, the binder is synthesized through the reaction of aluminosilicate materials with alkaline liquids. This geopolymer cement gel binds aggregates and unreacted materials, resulting in geopolymer concrete. Additional cementitious materials such as fly ash and slag are commonly used in geopolymer concrete, offering further environmental benefits.

The development of geopolymer binders as substitutes for OPC represents a significant advancement in concrete technology. Geopolymer is an inorganic aluminosilicate polymer synthesized from materials like fly ash, Metakaolin, or GGBS, through a polymerization mechanism involving alkaline solutions and aluminosilicate sources. Geopolymer constituents typically include fly ash and alkaline solutions, with sodium hydroxide and sodium silicate being

common choices due to their cost-effectiveness. Various terms such as alkali-activated cement, inorganic polymer concrete, and geo-cement have been used interchangeably to describe materials synthesized using similar chemistry to geopolymers. These innovations hold promise for reducing the environmental impact of concrete production while offering cost-effective alternatives to traditional OPC-based concrete.

ASTM C618-08a [1] identifies two types of fly ash: Class F and Class C, distinguished primarily by their calcium, silica, alumina, and iron content. Class F fly ash generally has a calcium content ranging from 1 to 12%, including calcium hydroxide, calcium sulfate, and glassy compounds mixed with silica and alumina. In contrast, Class C fly ash can contain up to 30% calcium oxide. The alkali activation process of fly ash involves an exothermic reaction that breaks down the fly ash structure, specifically disrupting the Si–O–Si and Al–O–Al covalent bonds in the activating solution. This reaction releases a significant amount of heat, leading to the formation of a solid, cement-like material with high mechanical strength [2]. According to [3], 63 million tons of fly ash were produced, but only 39% was repurposed beneficially, with a large portion ending up in landfills. Utilizing fly ash as a substitute for Portland cement in certain concrete applications could greatly benefit the global environment and promote sustainable infrastructure development.

The characteristics of fly ash-based geopolymer concrete have been highlighted in studies [4,-11]. These studies indicate that geopolymer concrete is a promising construction material, offering high compressive strength, minimal drying shrinkage, low creep, excellent sulfate resistance, and good acid resistance. Experimental findings show that geopolymer concrete structural elements like beams and columns perform similarly under stress to those made of OPC concrete. Other recent research [7, 12] supports these findings, noting that geopolymer concrete possesses engineering properties suitable for various construction applications. One ton of fly ash can produce about 2.5 cubic meters of high-quality geopolymer concrete, and the chemical costs involved are lower than the cost of one ton of Portland cement. However, a unique challenge with geopolymer concrete is its low strength development at ambient temperatures.

One-part geopolymer binders, also known as hybrid alkaline cements, represent a recent advancement in geopolymer production aimed at simplifying the process of using silicate solution-activated geopolymers. This method involves mixing aluminosilicate source materials with solid activators [13]. Unlike traditional geopolymer binders that use silicate solutions as activators, one-part mixtures incorporate solid activators into a dry mix, initiating the reaction when water is added, much like ordinary Portland cement. This approach avoids the use of corrosive and viscous solutions, facilitating the mass production of geopolymer concrete and enhancing its commercial viability, earning the nickname "just add water."

Efforts have been made to activate aluminosilicate materials with alkalis at elevated temperatures to create one-part mix binders. For instance, [14] developed systems by calcining kaolinite or halloysite with powdered hydroxides. Their specimens showed a strength of 1 MPa after 7 days, which was lower than typical two-part systems. Conversely, mechanical testing of hydrothermally treated samples revealed that these materials undergo significant structural and mineralogical changes, resulting in remarkable improvements in mechanical properties under hydrothermal conditions. A single day of hydrothermal treatment at 100 °C significantly enhanced mechanical strength from 1 MPa to 4 MPa.

Fly ash geopolymer develops strength slowly at ambient temperatures [15]. To achieve reasonable strength, curing temperatures of 40–75 °C are generally required [16], which poses challenges for practical construction. Researchers have explored ways to enhance the strength development of fly ash geopolymers by incorporating additives like ground granulated blast furnace slag, flue gas desulfurization gypsum, and Portland cement [15, 17, 18]. The reaction between anhydrous sodium metasilicate and water is exothermic at normal temperatures, and the heat generated can improve the mechanical properties of one-part geopolymer. This research focuses on studying the mechanical properties and microstructure of geopolymer activated with varying percentages of anhydrous sodium metasilicate granules. This knowledge is expected to aid in the understanding and future application of high-calcium fly ash one-part geopolymers. One-part geopolymers represent a significant advancement in geopolymer technology, first described in 2007 [14]. These binders are a newly introduced class designed to simplify the complexities of handling silicate solution-activated geopolymers. They are produced by blending aluminosilicate precursors with solid activators [13, 19].

Efforts have been made to activate aluminosilicates with alkalis at elevated temperatures to create one-part mix binders. [14] developed one-part mix systems by calcining kaolinite or halloysite with powdered hydroxides, resulting in a strength of 1 MPa after 7 days of curing, which is weaker than typical two-part mix systems. [20] synthesized one-part "just add water" geopolymer binders through alkali-thermal activation of red mud, rich in alumina and calcium. Calcining the red mud with sodium hydroxide pellets at 800°C decomposes the original silicate and aluminosilicate phases, promoting the formation of new compounds with hydraulic properties. They found that hydrating the "one-part geopolymer" produced zeolites and a disordered binder gel, achieving a compressive strength of 10 MPa after 7 days. Although the compressive strength was relatively low, they reported that red mud is an effective precursor for one-part geopolymer binders through heat and alkali-activation processes. Similarly, [21] synthesized one-part geopolymer binder by thermally treating low-quality kaolin with alkalis at 950°C, resulting in a binder with a strength of over 47 MPa.

Additionally, [22] created one-part geopolymer mixes using rice husk ash (RHA) and solid sodium aluminate. They found that water plays a crucial role in geopolymerization. Higher crystalline formation occurred in samples with high water content, like trends in conventional geopolymer systems. However, increasing water content generally reduced alkalinity, slowed the reaction process, and resulted in a more porous microstructure, which is undesirable. Recent heat treatment techniques for making one-part mix binders have achieved strengths comparable to two-part mix systems. However, the high temperatures required for these methods limit their commercial application and increase their environmental impact.

In recent decades, crude oil extraction has increased rapidly. The transportation and storage of crude oil inevitably results in substantial amounts of PS waste accumulating in oil storage tanks [2]. Various activities in the oil industry, such as drilling, production, and transportation, generate hazardous waste [12]. Both upstream and downstream operations in the oil industry produce significant amounts of oily sludge. Upstream activities include extracting, transporting, and storing crude oil, while downstream activities involve refining crude oil. The produced PS in the oil industry is classified as either simple oil or oil waste, depending on the proportion of solid materials and water within the oil residue [15]. PS contains a high volume of solid

residues and is very viscous, whereas simple oil has a lower water content [15]. PS is the most hazardous waste generated in petroleum refineries, consisting of a semisolid, pasty material made of sand (a mixture of clay, silica, and oxides) contaminated by oil, produced water, and chemicals used in oil manufacturing [12].

Crude oil, or petroleum, is a naturally occurring flammable liquid composed of a complex mixture of hydrocarbons of various molecular weights and other organic compounds. It is found in geological formations beneath the earth's surface [23]. Crude oil contains hydrocarbons such as aromatic hydrocarbons (including phenol, polyaromatic hydrocarbons [PAHs], benzene, toluene, ethylbenzene, and xylene [BTEX]), alkanes, organic compounds (such as sulfur, oxygen, and nitrogen), inorganic compounds (including suspended solids, water-soluble metals, and salts), cycloalkanes, and metals like vanadium, iron, copper, and nickel. The molecular composition varies widely between different formations [24, 25, 26]. The composition of petroleum sludge (PS) is complex and challenging to manage, involving suspended solids and oil-in-water or water-in-oil emulsions. PS contains hazardous substances, including polycyclic aromatic hydrocarbons, aromatic hydrocarbons [28], and other toxic, carcinogenic, or mutagenic compounds. PS is difficult to hydrate due to its high viscosity and typically contains about 55.13% water, 9.246% residues, 1.9173% asphaltenes, 23.19% light hydrocarbons, and 10.514% wax. It also has high concentrations of metals, such as 0.6% iron, 204 ppm vanadium, and 506 ppm nickel, making it highly destructive to the environment and harmful to organisms, necessitating careful management for ecological protection [29].

The chemical composition of PS varies greatly depending on the source of the crude oil (oil field) and the drilling and refining processes [21, 29]. PS is characterized by a high hydrocarbon content, ranging from 5% to 86.2%, and typically has a pH value between 6.5 and 7.5 [15]. It is a complex mixture containing significant amounts of solids, water, oil, hydrocarbons, and various toxic, carcinogenic, or mutagenic compounds. Generally, petroleum sludge is composed of 40-52% alkanes, 8-10% asphaltenes, 28-31% aromatic hydrocarbons, and 7-22.4% resins [8].

Review of Proximate and Ultimate Analysis of Petroleum Sludge

Table 1 reviews the structural components of petroleum sludge (PS), derived from various researchers' findings. The highest recorded moisture content of as-received PS was 59.86%, which exceeds the typical maximum range of 30-40% by mass [10]. The maximum percentage of volatile hydrocarbons (VHC) by weight was 88.50%, although there is significant variation in the values reported. For ash content, three researchers found similar values of 72.49%, 71.68%, and 71.20%. Another study noted a decrease in ash content to 61.19%. Additionally, a considerable range of ash content was observed, with values of 54.59%, 53.92%, and 51.99%, while the lowest reported ash content was 4.40% by weight. As reported by [8], a nonvolatile hydrocarbon content of 90.48%, whereas Hu [3] reported 73.10% by mass. The high heating value (HHV) of the PS was found to be 18.69% by weight, while the low heating value (LHV) was higher, at 43.10% by weight.

Table 1: Review of Proximate Analysis for PS.

S/N	MC ^{ar}	VHC	Ash	NVHC	FC	HHV ^{ar}	LHV ^d	Sources
1	26.89	18.51	44.97	nr	9.6	nr	35.17	[58]
2	26.30	31.70	31.6	nr	nr	nr	nr	[59]
3	3.23	11.36	61.19	nr	27.45	9.23	nr	[60]
4	3.10	88.50	-	nr	8.40	nr	43.1	[9]
5	26.55	51.19	42.27	nr	2.17	nr	8.5362	[61]
6	10.26	32.72	54.59	nr	2.43	nr	nr	[62]
7	1.62	21.33	71.68	nr	5.37	nr	nr	[62]
8	34.84	48.59	9.79	nr	6.78	nr	nr	[62]
9	6.28	60.05	20.98	nr	12.69	17.01	nr	[1]
10	1.76	1.12	6.64	90.48	nr	nr	nr	[57]
11	16.95	28.94	51.99	nr	2.12	nr	8.53	[63]
12	59.86	88.09	8.61	nr	3.30	nr	17.73	[64]
13	6.80	15.70	4.40	73.10	nr	nr	nr	[3]
14	4.85	22.58	71.20	nr	1.37	8.77	nr	[65]
15	1.51	21.73	72.49	nr	4.27	7.54	nr	[2]
16	34.84	48.59	9.79	nr	6.78	18.69	nr	[5]

17	15.31	29.63	53.92	nr	1.14	14.02	nr	[7]
----	-------	-------	-------	----	------	-------	----	-----

ar-as received sample of sludge, d-dried sample, nr- not reported. Moisture Content, Volatile Hydrocarbon, Ash, Nonvolatile Hydrocarbon, and Fixed Carbon were measured by wt. % while High Heating and Low Heating Value were also measured in (MJ/kg).

From Table 2, the carbon content in PS varies widely, ranging from 16.38 to 23.86 wt.%. Additionally, the carbon content can increase significantly, reaching between 33.16 and a maximum of 81.20 wt.%. In contrast, the hydrogen content is relatively consistent, with values ranging from 1.29 to 12.80 wt.%. The nitrogen content peaks at 5.97 wt.%, with other values closely clustered between 0.08 and 1.21 wt.%. The oxygen content also shows a broad range, with the highest value at 34.19 wt.% and the lowest at 2.47 wt.%. Finally, the sulfur content ranges from 0.20 to 3.16 wt.%

Table 0: Review of Ultimate Analysis of PS (wt. %).

S/N	Carbon	Hydrogen	Nitrogen	Oxygen	Sulfur	References
1	16.53	1.29	0.08	12.70	0.60	[60]
2	81.20	9.20	0.40	4.10	0.20	[9]
3	16.38	4.25	0.32	8.91	2.34	[61]
4	23.86	3.07	1.16	15.25	3.16	[62]
5	18.80	2.69	0.28	6.05	0.65	[62]
6	42.45	8.07	1.21	30.34	1.42	[62]
7	60.70	12.80	0.80	28.90	1.00	[67]
8	40.81	4.60	5.97	20.32	1.05	[1]
9	20.85	2.70	1.40	6.00	0.11	[63]
10	33.16	7.18	0.45	nr	0.68	[64]
11	75.09	5.35	1.58	16.22	1.76	[3]
12	19.41	2.73	0.33	4.10	0.63	[65]
13	18.18	2.73	0.22	8.13	0.64	[65]
14	44.84	8.58	1.16	34.19	1.63	[65]
15	23.28	3.54	0.19	2.47	1.29	[66]
16	81.84	13.61	0.75	1.56	2.24	[58]

Technology of geopolymers

Hills of limestone are extensively mined for cement production, resulting in about 1.6 billion tons of material extracted annually, which leads to ecological imbalance, climate change, and adverse human health effects due to greenhouse gas emissions such as SO₂, CO₂, and dioxin [130]. According to the International Energy Agency (IEA), ordinary Portland cement (OPC) accounts for 10% of global greenhouse gas emissions. Cement production is projected to increase by 12% to 23% by 2050, potentially exacerbating the negative impacts on living species and the environment. The manufacture of OPC inherently involves substantial CO₂ emissions: first, from burning fuels to achieve the high temperatures needed in kilns, and second, from heating limestone through the calcining process.

As OPC is widely used as a binding material, the pressure on raw material resources has prompted construction companies to seek alternative binders. Recently, the use of agricultural and industrial waste products has gained attention due to the health risks and high costs associated with their disposal. Using these waste products in cement production addresses some issues but the increasing demand for cement highlights its significant impact on global warming due to CO₂ emissions. This has led researchers to explore the potential of aluminosilicate precursors activated with alkaline solutions as a replacement for traditional cement.

Geopolymers have emerged as a promising solution for the safe and effective disposal of solid waste. The term "geopolymer" was introduced by French scientist Joseph Davidovits in 1978. Geopolymers are inorganic polymers created by reacting alumina-rich and silica-rich materials with a highly alkaline solution, combining properties of ceramics, polymers, and cement [11]. Figure 2.8 illustrates the production of clean geopolymer mortar or concrete using by-products and an alkaline solution. Over the past few decades, researchers have focused on developing geopolymer products using various low-cost aluminosilicate materials with a three-dimensional amorphous microstructure, or other industrial by-products (e.g., rice husk ash, fly ash, furnace slag), activated with alkaline solutions [12].

Compressive Strength

The compressive strength of geopolymer mortar or concrete is a crucial property for construction and quality assurance, indicating the maximum compression force the material can withstand without failure. This strength serves as a general measure of mortar or concrete quality and is an important indicator of other properties. The compressive strength of geopolymer mortar is typically measured according to ASTM C109/C109M standards. According to the European standard EN 206-1 [215], the required 28-day compressive strength for different concrete categories ranges from 8 to 100 MPa for lightweight concrete and 10 to 115 MPa for ordinary concrete. Specific ranges for lightweight concrete are from 8 to 80 MPa and 9 to 88 MPa, respectively.

Variations in the compressive strength of fly ash-based geopolymer mortar can be attributed to factors such as the size distribution, shape, and amorphous microstructure of the aluminosilicate materials used [168]. In this process, the aluminum and silicon components of fly ash are activated by alkaline solutions, leading to polymerization into atomic chains that form a binder, which binds the fine and coarse aggregates into a homogeneous matrix. This matrix achieves maximum strength at elevated temperatures. The calcium content in fly ash plays a significant role in strength development; however, low-calcium fly ash is preferred for binding properties because geopolymer binders depend on the silicon and aluminum content of the source materials for optimal performance.

The compressive strength of geopolymer products is also influenced by the concentration of the alkaline solution, with higher concentrations leading to increased strength. Other factors affecting the strength of geopolymer mortar include the binder-to-aggregate ratio, the ratio of sodium silicate to sodium hydroxide, the molarity of sodium hydroxide, the solution-to-binder ratio, the ratio of silicate to sodium oxide, the silicate-to-aluminum ratio, and the calcium content [36]. Adding fly ash, silica fume, and kaolin to geopolymer concrete can enhance compressive strength up to a certain point, but excessive kaolin reduces strength. Additionally, incorporating slag improves strength by densifying the matrix through the filling of void spaces, resulting in a finer surface and increased compressive strength. Overall, the compressive strength is significantly influenced by the calcium content in the precursor materials, the concentration of sodium hydroxide (NaOH), and the ratio of sodium silicate to sodium hydroxide.

Calcium Content Effect

[37] investigated the impact of granulated blast furnace slag (GBFS) and varying levels of metakaolin (MK) on the compressive strength of geopolymer mortar. They incorporated MK at 0%, 5%, 10%, and 15% levels. Their findings showed that the compressive strength at 28 days increased with higher MK content, rising from 42 MPa to 63.1 MPa. Figure 2 illustrates how different levels of MK replacement affect the compressive strength development of geopolymer mortars.

Additionally, Figure 2 demonstrates the influence of the calcium-to-silicate ratio on compressive strength under various curing conditions, including different temperatures and curing times. The research revealed that compressive strength decreased with higher curing temperatures and lower calcium-to-silicate ratios. Specifically, a low compressive strength was observed with a calcium-to-silicate ratio of 1.08 at a curing temperature of 90°C under oven curing conditions [38].

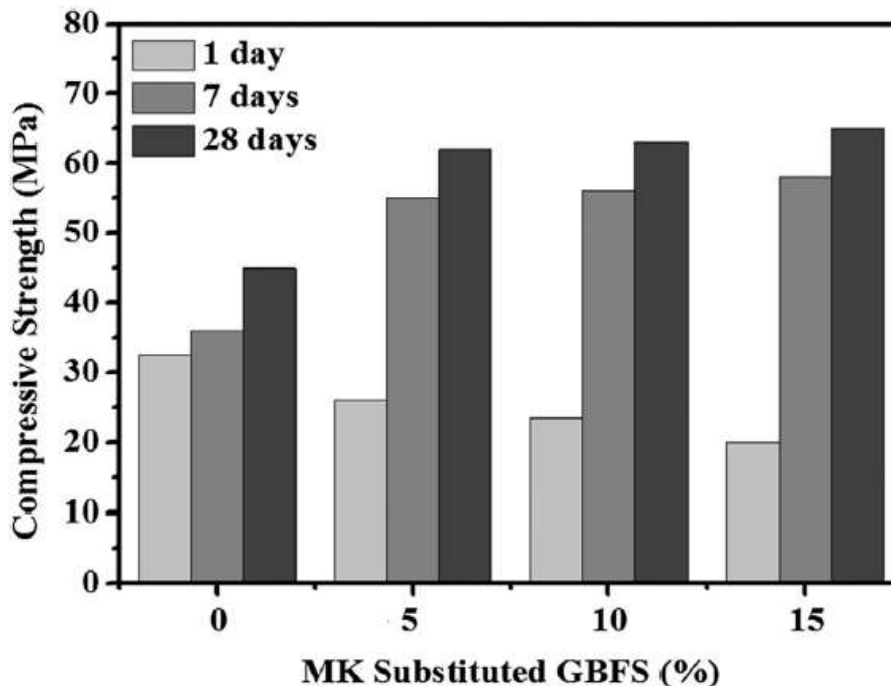


Figure 1: Effect of MK replaced GBFS on compressive strength development of geopolymer mortar [26].

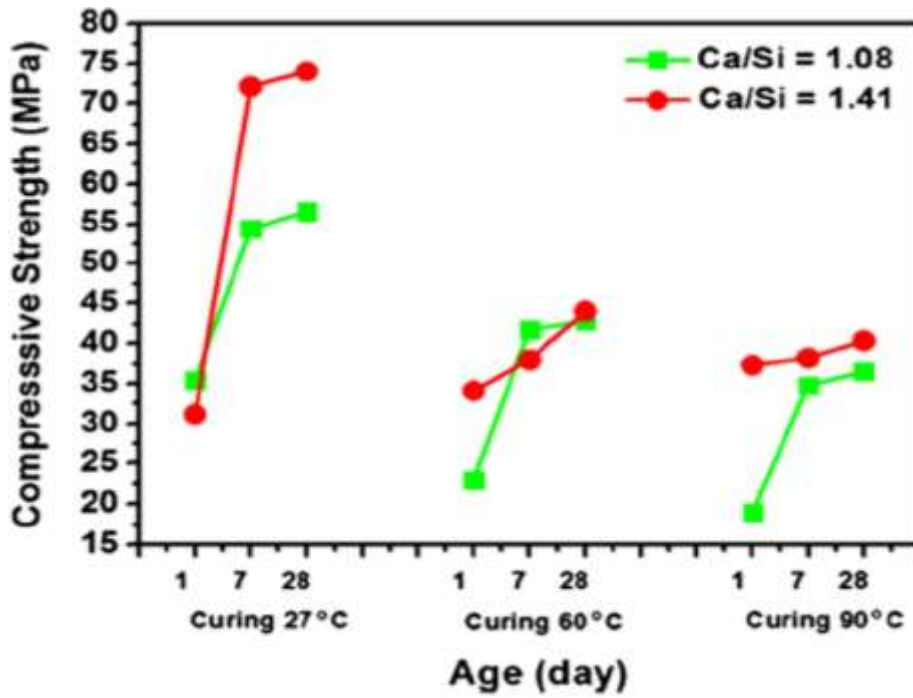


Figure 0: Impact of Ca/Si ratios on compressive strength at various durations and curing temperatures [27].

Effect of Sodium Hydroxide Molarity

[28] investigated how varying sodium hydroxide concentrations (6, 10, and 14 M) influenced the development of compressive strength in geopolymer mortar. Their findings indicated that an increase in molarity led to a corresponding increase in compressive strength. Similarly, Vasconcelos et al. [20] examined the impact of different sodium hydroxide concentrations (12, 14, and 16 M) on the strength of geopolymer mortar. Their results showed that compressive strength improved as the molarity increased from 12 to 14 M after 7, 28, and 56 days of curing. However, at 16 M, the compressive strength was observed to be lower than that at 14 M, as depicted in Figure 3.

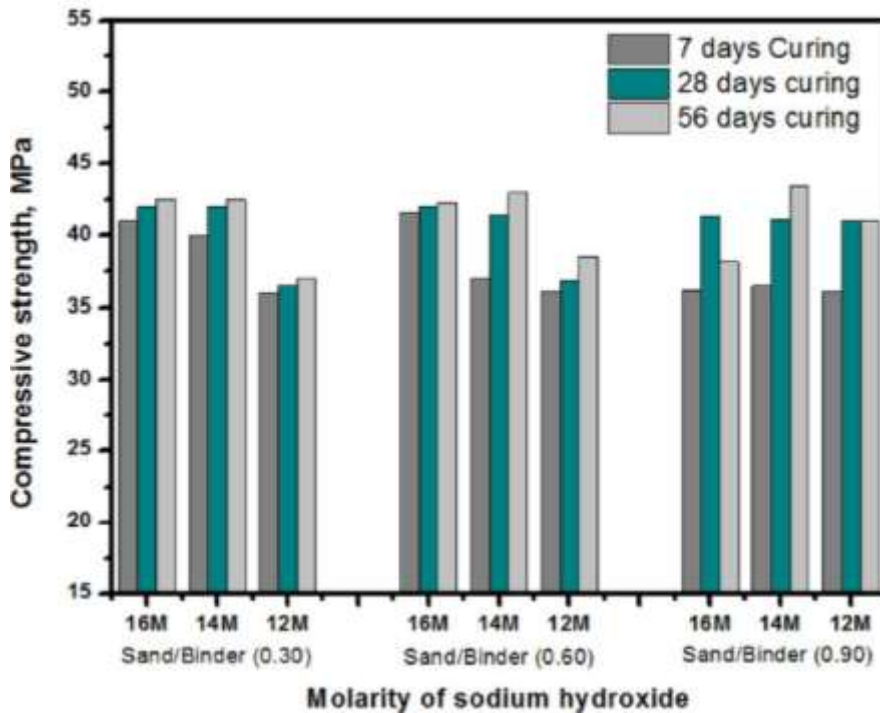


Figure 3: Compressive strength development of geopolymer mortar vs. concentration of sodium hydroxide at different curing days with the inclusion of various sand to binder mass ratios (30%, 60%, and 90%) [20].

Flexural Strength

The flexural strength of geopolymer mortar/concrete is crucial for understanding the structural behavior under service loads. This strength depends on the matrix microstructure and the transition zone between the cement paste and aggregate. It is particularly significant in the design of reinforced concrete structures. Typically, the flexural strength of geopolymer binders is measured using the three-point bending test, as reported in the literature. The failure of tension in OPC/geopolymer concrete is characterized by micro-cracking, especially in the transition region of interfaces. The physical characteristics of this transition zone affect flexural strength more significantly than compressive strength.

For mortars made with ordinary Portland cement (OPC), those with maximum compressive strength often have optimal flexural strength. However, geopolymer mortar exhibits high flexural strength despite lower compressive strength due to the excellent adhesion of the paste to sand particles and the inherent brittleness of the geopolymer mortar. The sand content significantly influences the flexural strength of geopolymer mortars. [31] reported that increasing sand content could enhance the flexural strength, with optimal strength achieved at 78% sand content. Beyond this point, flexural strength declines due to insufficient binder among sand particles, leading to void spaces and increased porosity.

Figure 3 illustrates the effect of ground granulated blast furnace slag (GGBFS) on the flexural strength of fly ash-based geopolymer mortar. The figure shows that adding GGBFS increases flexural strength at all curing times, with a more noticeable increase at 7 days (approximately 221%) compared to 28 days (80%) with GGBFS content from 10% to 40%. Geopolymer mortar made with 95% GGBFS and 5% metakaolin achieved a high early flexural strength of 5.7 MPa, surpassing ordinary Portland cement-based mortar. Additionally, the 28-day flexural strength exceeded 8 MPa, a more than 50% improvement over ordinary Portland cement mortar. These findings highlight the early strength gains of high-calcium binders due to C–S–H formation, like alkali-activated mortars, unlike OPC which relies solely on C–S–H formation. However, the early flexural strength of geopolymer mortar made with GGBFS and fly ash decreases with increasing curing temperatures from 27°C to 90°C due to heat-induced micro-cracks.

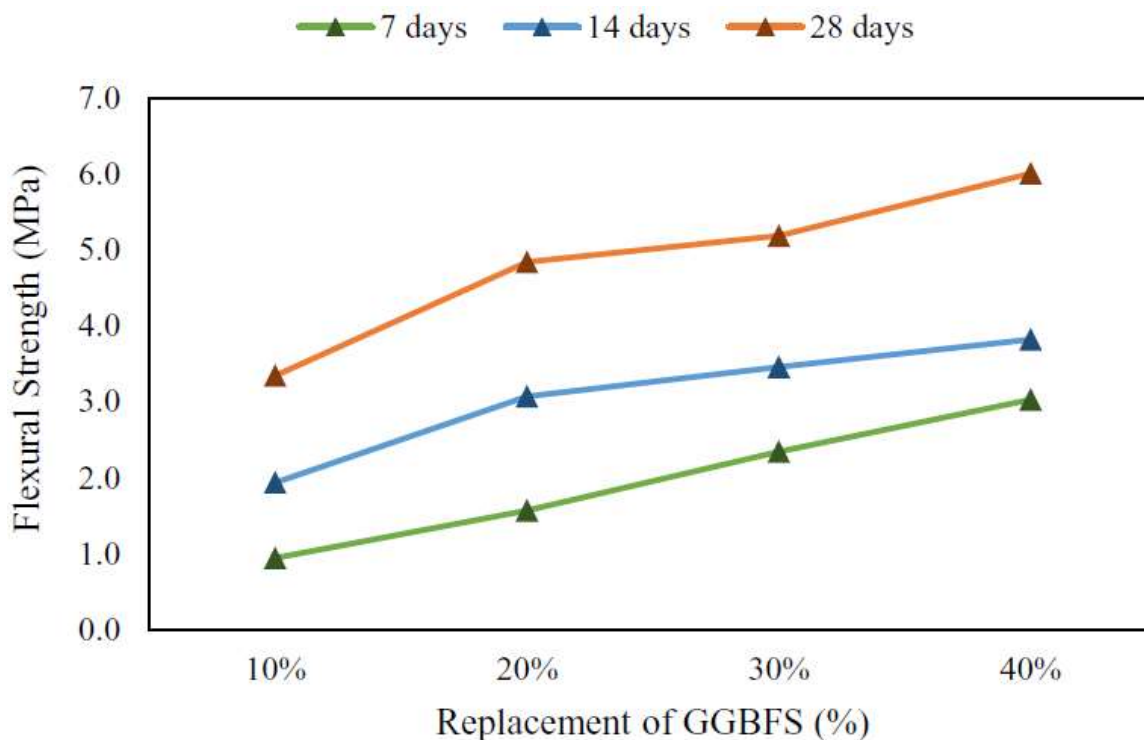


Figure 4: Effect of GGBFS replacement on flexural strength of FA/GGBFS mortar [25].

X-Ray Diffraction (XRD) Technique

[22] analyzed the XRD patterns of fly ash and geopolymer, as shown in Figure 2.27. The fly ash exhibited an amorphous phase, characterized by a broad hump around $2\theta = 20^\circ\text{--}38^\circ$. This amorphous structure is typical of aluminosilicate materials, though other peaks were also observed. In the geopolymer, these broad humps persisted, indicating that the amorphous structure of the aluminosilicate was maintained.

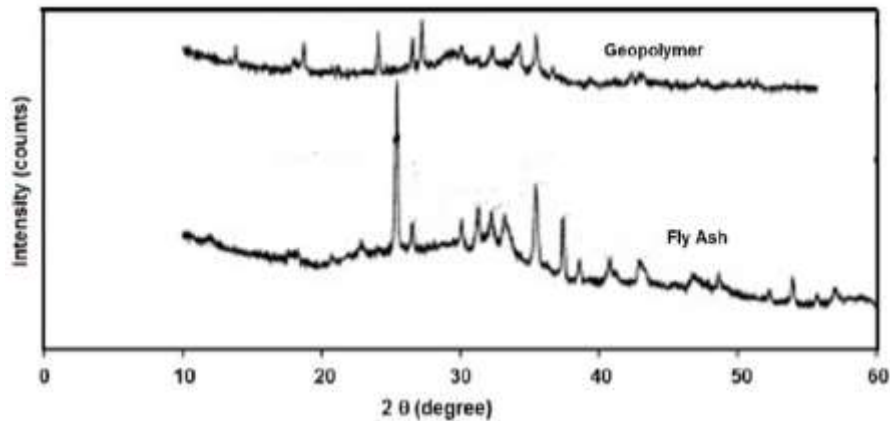


Figure 5: XRD pattern of fly ash and geopolymer [22].

Results and Discussions

Compressive Strength of Geopolymer Mortar

The unconfined compressive strength (UCS) of geopolymer mortar samples, varying by PSA percentage, sodium silicate to sodium hydroxide ratios, and sodium hydroxide concentrations, was measured at 3, 7, and 28 days (Figure 4.8). As expected, compressive strength increased with curing time from 3 to 28 days, likely due to the ongoing geopolymerization reaction.

At 3 days, the reference control geopolymer mortar exhibited higher strength than those containing 10% and 20% PSA, attributed to the alkali in the matrix promoting early geopolymerization. The 3-day UCS of reference mortar M3 was 25% higher than M11, and M4 was 13.83% higher than M7, due to the low early pozzolanic reaction of PSA. However, control mortar M6 had lower strength than mortars with 10% and 20% PSA by 58.7% and 20.90%, respectively. At 7 days, compressive strength improved significantly across all 20 mixtures. By 28 days, M11 had a compressive strength 9.38% higher than M3, and M14 and M19 were 8.66% and 11.18% higher than M6, respectively.

Incorporating 20% PSA activated with sodium silicate and sodium hydroxide enhanced compressive strength, likely due to the PSA particles reacting in the matrix, continuing the geopolymerization process, and forming a dense, three-dimensional calcium aluminosilicate hydrate gel (C–A–S–H). The molarity of sodium hydroxide had a greater effect on compressive strength than the sodium silicate to sodium hydroxide ratio. Formation of sodium carbonate was observed on the surface of cubes made with 16 molarity sodium hydroxide, attributed to excess Na^+ cations reacting with atmospheric CO_2 , forming efflorescence like $\text{Na}_2\text{CO}_3 \cdot \text{H}_2\text{O}$ and $\text{Na}_2(\text{HCO}_3)(\text{CO}_3) \cdot 2\text{H}_2\text{O}$ under curing humidity conditions .

Compressive strength plot of geopolymer mortar.

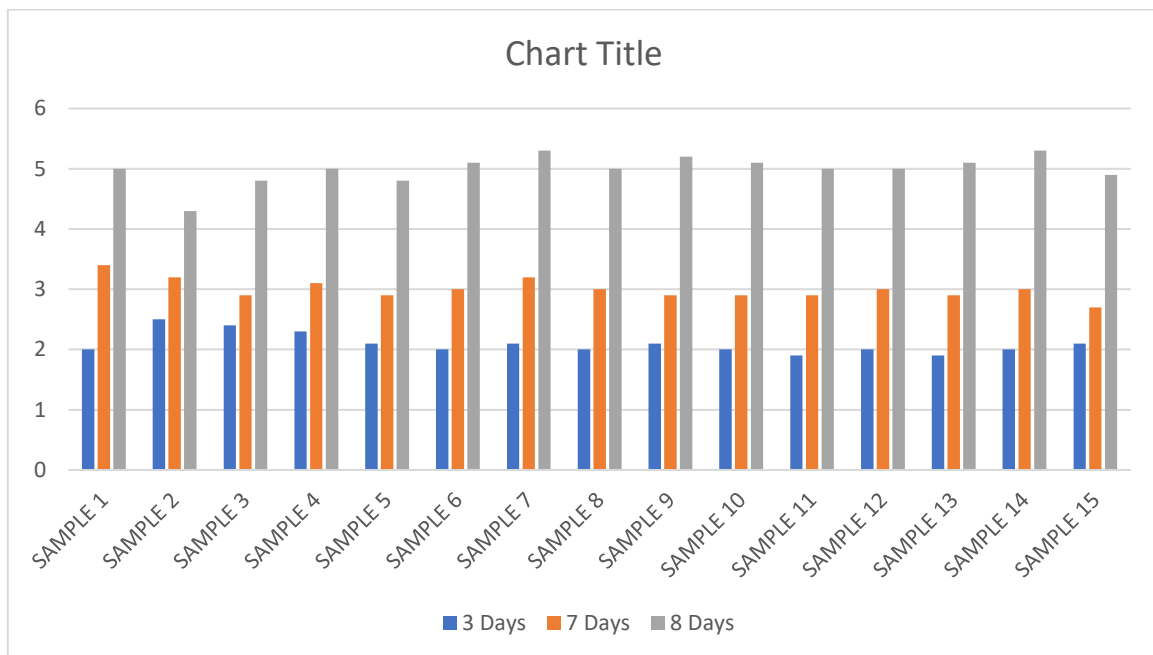


Figure 4, Compressive strength results

Figure 4.8 illustrates the unconfined compressive strength (UCS) of geopolymer mortar samples with varying percentages of PSA, different sodium silicate to sodium hydroxide ratios, and sodium hydroxide concentrations at 3, 7, and 28 days. As anticipated, all geopolymer mortar mixtures exhibited increased compressive strength with prolonged curing from 3 to 28 days. This increase is likely due to the ongoing geopolymerization reaction over time, enhancing the strength.

At the 3-day mark, the reference control geopolymer mortar showed higher strength compared to those with 10% and 20% PSA, attributed to the presence of alkali that accelerates geopolymerization early on. As shown in Figure A, the UCS of reference mortar M3 was 25% higher than mortar M11. Similarly, M4 was 13.83% stronger than M7. The lower strength of the geopolymer mortars with PSA at an early age is due to the slow pozzolanic reaction of PSA. However, control mortar M6 had lower strength than mortars with 10% and 20% PSA by 58.7% and 20.90%, respectively.

By 7 days, all 20 geopolymer mortar mixtures showed significant strength improvements. At 28 days, mortar M11 had a 9.38% higher compressive strength than control M3, and mortars M14 and M19 exceeded control M6 by 8.66% and 11.18%, respectively.

Incorporating 20% PSA activated with sodium silicate and sodium hydroxide increased compressive strength, likely due to PSA particles reacting within the geopolymer matrix, the continued geopolymerization process, and the multi-condensation of aluminosilicate forming a three-dimensional structure. This process also produced calcium aluminosilicate hydrate gel (C–A–S–H) from the calcium in the source materials, creating dense, compact mortar structures as seen in micrographs, thereby enhancing mechanical performance.

The compressive strength profile indicates that sodium hydroxide molarity has a more significant impact than the sodium silicate to sodium hydroxide ratio. On the surface of geopolymer mortar cubes made with 16 molarity sodium hydroxide, sodium carbonate formation was observed. This is due to excess Na⁺ cations moving inside the pore structure and reacting with atmospheric carbon dioxide after water evaporation. Efflorescence in geopolymers, such as Na₂CO₃·H₂O and Na₃(HCO₃)(CO₃)·2H₂O, was noted, with the extent and nature of efflorescence being influenced by curing humidity conditions.

REFERENCES

- [1] S. Deng *et al.*, "Experimental and modeling study of the long cylindrical oily sludge drying process," *Applied Thermal Engineering*, vol. 91, pp. 354-362, 2015, doi: 10.1016/j.applthermaleng.2015.08.054.
- [2] W. Xiao, X. Yao, and F. Zhang, "Recycling of Oily Sludge as a Roadbed Material Utilizing Phosphogypsum-Based Cementitious Materials," *Advances in Civil Engineering*, vol. 2019, pp. 1-10, 2019, doi: 10.1155/2019/6280715.
- [3] J. Hu *et al.*, "Extraction of crude oil from petrochemical sludge: Characterization of products using thermogravimetric analysis," *Fuel*, vol. 188, pp. 166-172, 2017, doi: 10.1016/j.fuel.2016.09.068.
- [4] D. Ramirez and C. D. Collins, "Maximisation of oil recovery from an oil-water separator sludge: Influence of type, concentration, and application ratio of surfactants," *Waste Manag*, vol. 82, pp. 100-110, Dec 2018, doi: 10.1016/j.wasman.2018.10.016.
- [5] I. Fitri, Ni'matuzahroh, and T. Surtiningsih, "Bioremediation of oil sludge using a type of nitrogen source and the consortium of bacteria with composting method," 2017.
- [6] M. A. Nazem and O. Tavakoli, "Bio-oil production from refinery oily sludge using hydrothermal liquefaction technology," *The Journal of Supercritical Fluids*, vol. 127, pp. 33-40, 2017, doi: 10.1016/j.supflu.2017.03.020.
- [7] X. Wang, Q. Wang, S. Wang, F. Li, and G. Guo, "Effect of biostimulation on community level physiological profiles of microorganisms in field-scale biopiles composed of aged oil sludge," *Bioresour Technol*, vol. 111, pp. 308-15, May 2012, doi: 10.1016/j.biortech.2012.01.158.
- [8] A. Aguelmous *et al.*, "Petroleum sludge bioremediation and its toxicity removal by landfill in gunder semi-arid conditions," *Ecotoxicol Environ Saf*, vol. 166, pp. 482-487, Dec 30 2018, doi: 10.1016/j.ecoenv.2018.09.106.
- [9] B. Lin, Q. Huang, and Y. Chi, "Co-pyrolysis of oily sludge and rice husk for improving pyrolysis oil quality," *Fuel Processing Technology*, vol. 177, pp. 275-282, 2018, doi: 10.1016/j.fuproc.2018.05.002.
- [10] B. Lin, J. Wang, Q. Huang, and Y. Chi, "Effects of potassium hydroxide on the catalytic pyrolysis of oily sludge for high-quality oil product," *Fuel*, vol. 200, pp. 124-133, 2017, doi: 10.1016/j.fuel.2017.03.065.
- [11] Y. Shen, X. Chen, J. Wang, X. Ge, and M. Chen, "Oil sludge recycling by ash-catalyzed pyrolysis-reforming processes," *Fuel*, vol. 182, pp. 871-878, 2016, doi: 10.1016/j.fuel.2016.05.102.
- [12] L. J. da Silva, F. C. Alves, and F. P. de Franca, "A review of the technological solutions for the treatment of oily sludges from petroleum refineries," *Waste Manag Res*, vol. 30, no. 10, pp. 1016-30, Oct 2012, doi: 10.1177/0734242X12448517.
- [13] E. N. Pakpahan, M. H. Isa, S. R. Kutty, S. Chantara, and W. Wiriyana, "Polycyclic aromatic hydrocarbon removal from petroleum sludge cake using thermal treatment with additives," *Environ Technol*, vol. 34, no. 1-4, pp. 407-16, Jan-Feb 2013, doi: 10.1080/09593330.2012.698648.
- [14] J. Oladejo, K. Shi, X. Luo, G. Yang, and T. Wu, "A Review of Sludge-to-Energy Recovery Methods," *Energies*, vol. 12, no. 1, 2018, doi: 10.3390/en12010060.

- [15] G. Hu, J. Li, and G. Zeng, "Recent development in the treatment of oily sludge from petroleum industry: a review," *J Hazard Mater*, vol. 261, pp. 470-90, Oct 15 2013, doi: 10.1016/j.jhazmat.2013.07.069.
- [16] E. Pakpahan, N. Shafiq, M. Isa, S. Kutty, and M. Mustafa, "Petroleum sludge thermal treatment and use in cement replacement – A solution towards sustainability," in *Civil, Offshore and Environmental Engineering*, 2016, pp. 251-256.
- [17] R. Malviya and R. Chaudhary, "Factors affecting hazardous waste solidification/stabilization: a review," *J Hazard Mater*, vol. 137, no. 1, pp. 267-76, Sep 1 2006, doi: 10.1016/j.jhazmat.2006.01.065.
- [18] S. Liang, J. Chen, M. Guo, D. Feng, L. Liu, and T. Qi, "Utilization of pretreated municipal solid waste incineration fly ash for cement-stabilized soil," *Waste Manag*, vol. 105, pp. 425-432, Mar 15 2020, doi: 10.1016/j.wasman.2020.02.017.
- [19] C. Pan, X. Xie, J. Gen, and W. Wang, "Effect of stabilization/solidification on mechanical and phase characteristics of organic river silt by a stabilizer," *Construction and Building Materials*, vol. 236, 2020, doi: 10.1016/j.conbuildmat.2019.117538.
- [20] A. M. Ali *et al.*, 2017, doi: 10.20944/preprints201708.0033.v1.
- [21] P. Devi, P. Kothari, and A. K. Dalai, "Stabilization and solidification of arsenic and iron contaminated canola meal biochar using chemically modified phosphate binders," *J Hazard Mater*, vol. 385, p. 121559, Mar 5 2020, doi: 10.1016/j.jhazmat.2019.121559.
- [22] L. E. Gordon, J. L. Provis, and J. S. J. Van Deventer, "Non-traditional ("geopolymer") cements and concretes for construction of large CCS equipment," *Energy Procedia*, vol. 4, pp. p. 2058-2065, 2011.
- [23] N. Xu, W. Wang, P. Han, and X. Lu, "Effects of ultrasound on oily sludge deoiling," *J Hazard Mater*, vol. 171, no. 1-3, pp. 914-7, Nov 15 2009, doi: 10.1016/j.jhazmat.2009.06.091.
- [24] O. R. S. da Rocha, R. F. Dantas, M. M. M. B. Duarte, M. M. L. Duarte, and V. L. da Silva, "Oil sludge treatment by photocatalysis applying black and white light," *Chemical Engineering Journal*, vol. 157, no. 1, pp. 80-85, 2010, doi: 10.1016/j.cej.2009.10.050.
- [25] R. Kemp, E. Barteková, and S. Türkeli, "The innovation trajectory of eco-cement in the Netherlands: a co-evolution analysis," *International Economics and Economic Policy*, vol. 14, no. 3, pp. 409-429, 2017, doi: 10.1007/s10368-017-0384-4.
- [26] A. Teklay, C. Yin, and L. Rosendahl, "Flash calcination of kaolinite rich clay and impact of process conditions on the quality of the calcines: A way to reduce CO2 footprint from cement industry," *Applied Energy*, vol. 162, pp. 1218-1224, 2016, doi: 10.1016/j.apenergy.2015.04.127.
- [27] D.-Y. Oh, T. Noguchi, R. Kitagaki, and W.-J. Park, "CO2 emission reduction by reuse of building material waste in the Japanese cement industry," *Renewable and Sustainable Energy Reviews*, vol. 38, pp. 796-810, 2014, doi: 10.1016/j.rser.2014.07.036.
- [28] X. Y. Zhuang *et al.*, "Fly ash-based geopolymer: clean production, properties and applications," *Journal of Cleaner Production*, vol. 125, pp. 253-267, 2016, doi: 10.1016/j.jclepro.2016.03.019.
- [29] T. W. Cheng and J. P. Chiu, "Fire-resistant geopolymer produced by granulated blast furnace slag," *Minerals Engineering*, vol. 16, no. 3, pp. 205-210, 2003, doi: 10.1016/s0892-6875(03)00008-6.
- [30] S. Wang, "Compressive strengths of mortar cubes from hydrated lime with cofired biomass fly ashes," *Construction and Building Materials*, vol. 50, pp. 414-420, 2014, doi: 10.1016/j.conbuildmat.2013.09.045.
- [31] H.-C. Wu and P. Sun, "New building materials from fly ash-based lightweight inorganic polymer," *Construction and Building Materials*, vol. 21, no. 1, pp. 211-217, 2007, doi: 10.1016/j.conbuildmat.2005.06.052.
- [32] P. Bankowski, L. Zou, and R. Hodges, "Reduction of metal leaching in brown coal fly ash using geopolymers," *J Hazard Mater*, vol. 114, no. 1-3, pp. 59-67, Oct 18 2004, doi: 10.1016/j.jhazmat.2004.06.034.
- [33] "<Recycling of Industrial Wastewater by Its Immobilization in Geopolymer Cement.pdf>."
- [34] "<Development of geopolymeric materials from industrial solid wastes.pdf>."
- [35] m. Dohim, A. Abdelaal, M. Beheary, N. Abdullah, and t. A. Razek, "Compressive strength of geopolymeric cubes produced from solid wastes of Alum Industry and Drinking Water Treatment Plants," *Egyptian Journal of Chemistry*, vol. 0, no. 0, pp. 0-0, 2019, doi: 10.21608/ejchem.2019.12745.1790.
- [36] G. Fahim Huseien, J. Mirza, M. Ismail, S. K. Ghoshal, and A. Abdulameer Hussein, "Geopolymer mortars as sustainable repair material: A comprehensive review," *Renewable and Sustainable Energy Reviews*, vol. 80, pp. 54-74, 2017, doi: 10.1016/j.rser.2017.05.076.
- [37] "<1-s2.0-S0026265X98916010-main.pdf>."
- [38] "METHOD 1311 TOXICITY CHARACTERISTIC LEACHING PROCEDURE."
- [39] "<40-C027.pdf>."

[40] O. C. Aja, H. H. Al-Kayiem, M. G. Zewge, and M. S. Joo, "Overview of Hazardous Waste Management Status in Malaysia," in *Management of Hazardous Wastes*, 2016, ch. Chapter 5.